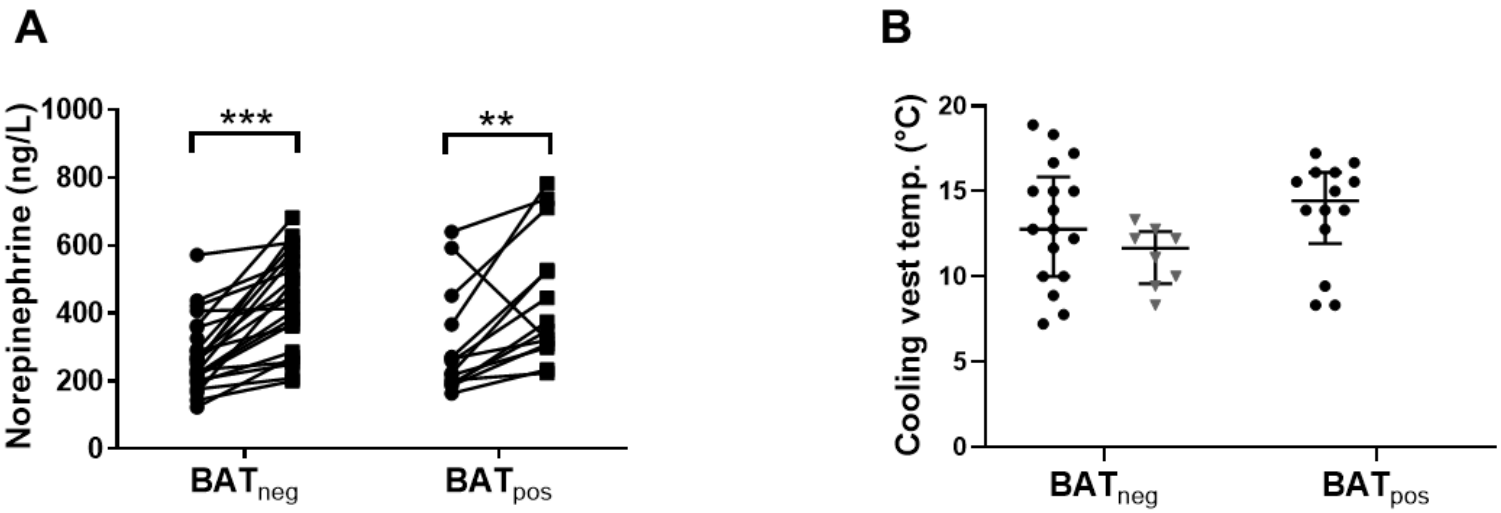

Supplementary Figure 1: No difference in the adrenergic response or cooling temperatures between BAT_{neg} and BAT_{pos} participants. Individual norepinephrine levels before and after cold exposure (A). Difference in the water temperatures of the cooling vests comparing BAT_{neg} and BAT_{pos} individuals (women = dots, men = inverted triangles) (B). *$p < 0.050$, **$p \leq 0.010$, ***$p \leq 0.001$

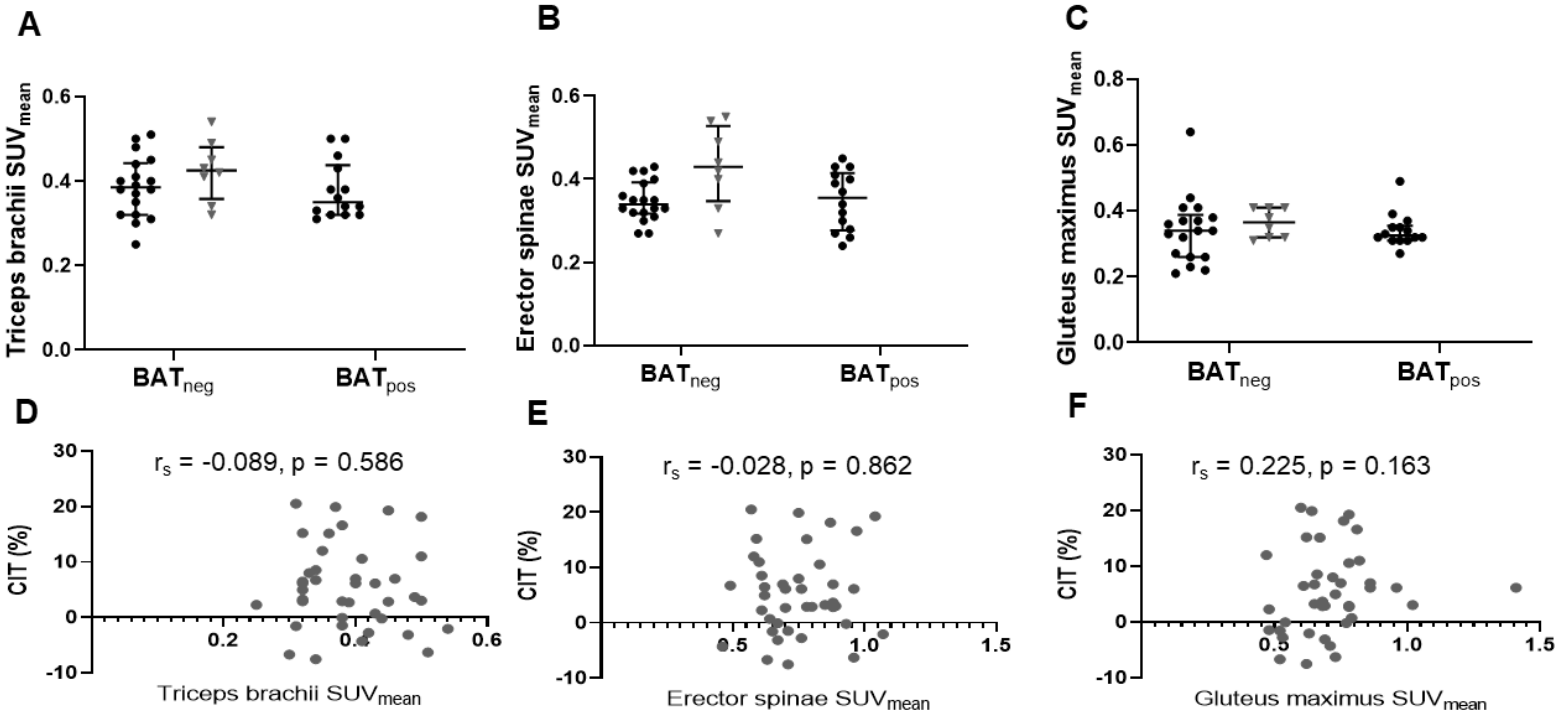

Supplemental Figure 2: No association of skeletal muscle glucose uptake with BAT status or cold-induced thermogenesis (CIT). Comparison of ^{18}F-FDG uptake in triceps brachii (A), erector spinae (B) and gluteus maximus (C). Dot plots for the associations between CIT and ^{18}F-FDG uptake uptake in triceps brachii (D), erector spinae (E), as well as gluteus maximus (F). In panels A-C women are depicted by dots and men by inverted triangles. r_s= Spearman‘s rank correlation coefficient.

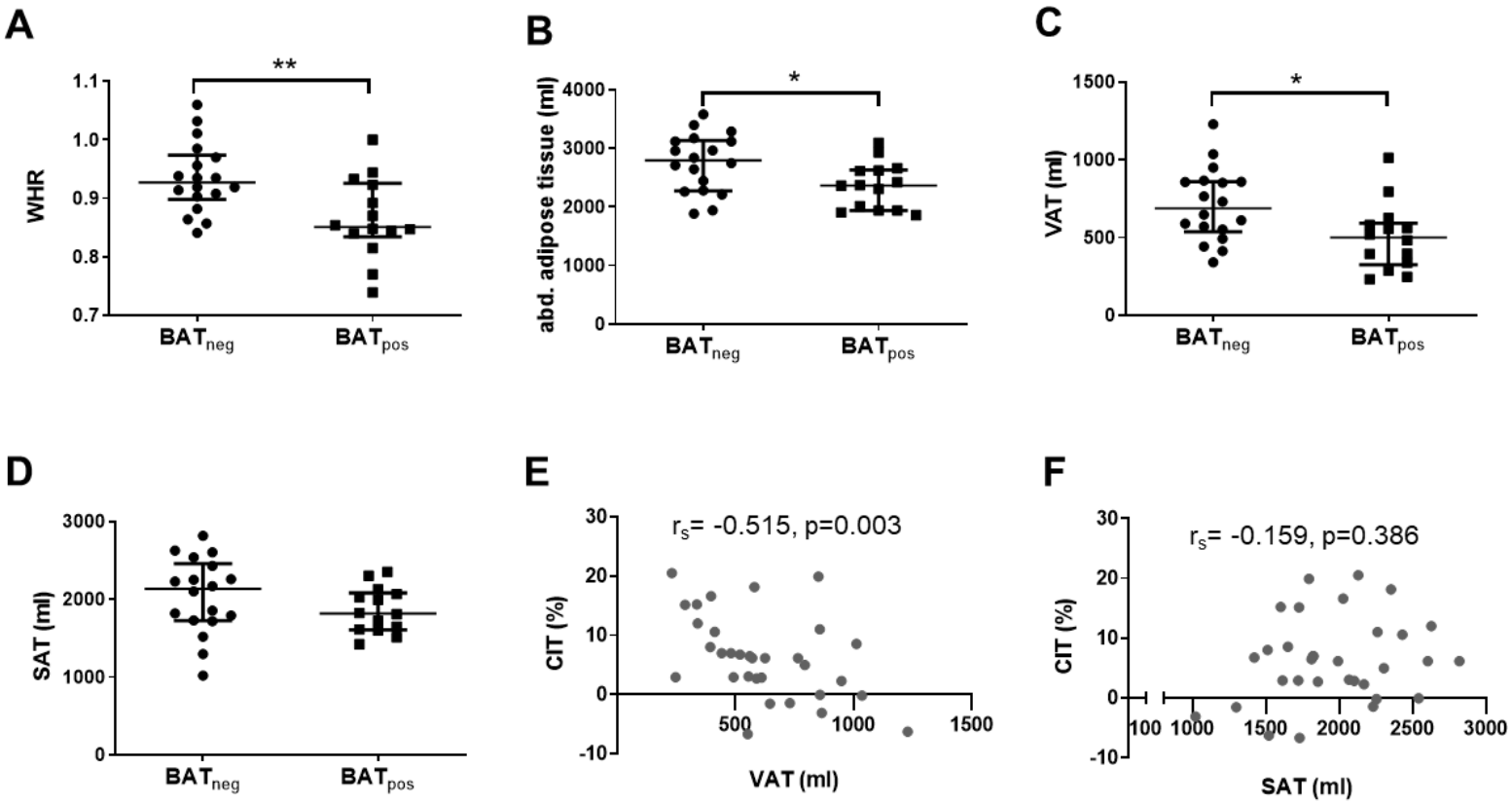

Supplemental Figure 3: Inverse association between visceral obesity and BAT glucose uptake as well as cold-induced thermogenesis (CIT) in women. Waist-to-hip ratio (WHR) (A), total abdominal adipose tissue volume (B), visceral adipose tissue (VAT) volume (C), and abdominal subcutaneous adipose tissue (SAT) volume (D) in BAT_{pos} versus BAT_{neg} women. VAT volume (E) but not SAT volume (F) is inversely associated with CIT in women. r_s= Spearman's rank correlation coefficient. *p < 0.050, **p≤0.010, ***p ≤0.001.

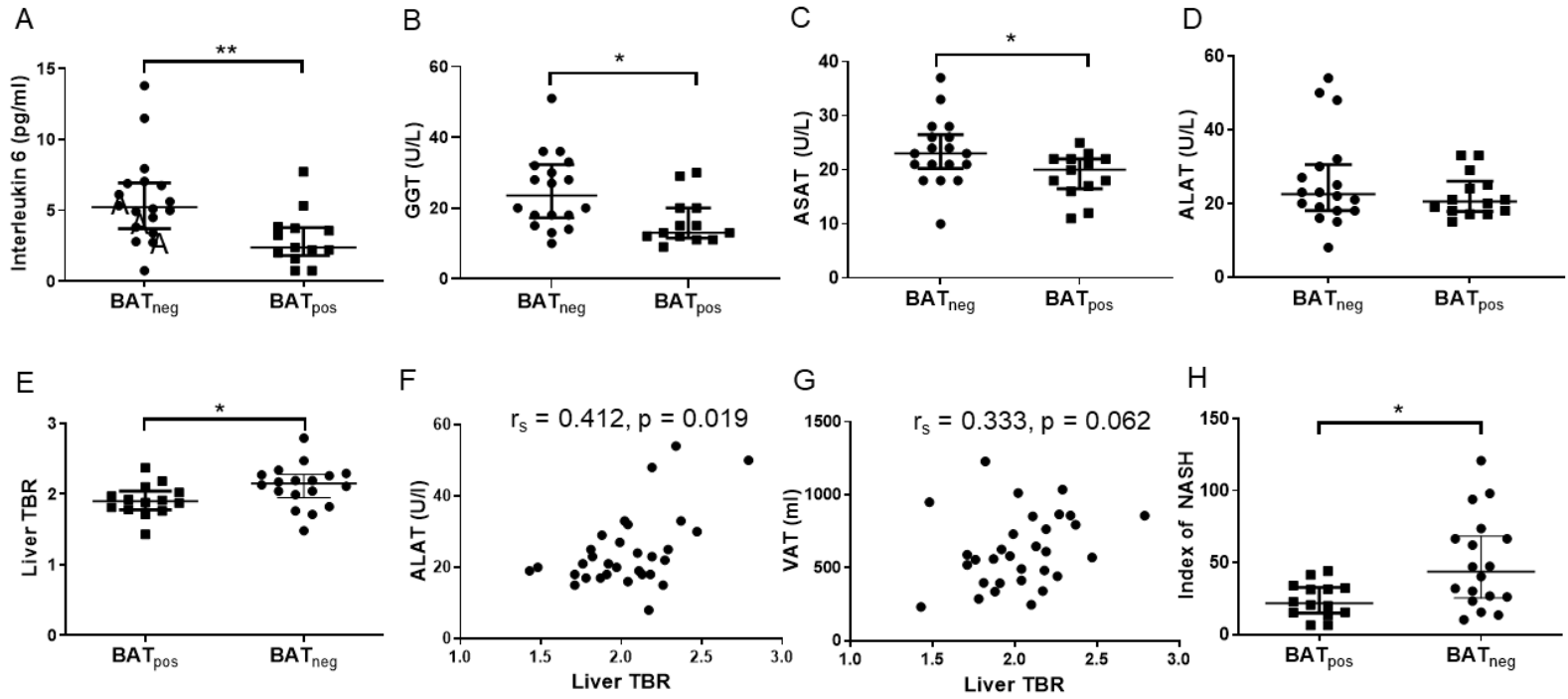

Supplemental Figure 4: In women, active BAT is associated with improved NAFLD parameters and reduced inflammation. Dot plots for interleukin 6 (IL-6) (A), gamma-glutamyltransferase (GGT) (B), aspartate aminotransferase (ASAT) (C), alanine aminotransferase (ALAT) (D), Liver target-to-background ratio (TBR) (E), and Index of NASH (ION) (H). comparing BAT_{neg} and BAT_{pos} women. The scatterplots depict the associations between liver TBR and ALAT (F) as well as between liver TBR and visceral adipose tissue (VAT) volume (G).*$p < 0.050$, **$p \leq 0.010$, ***$p \leq 0.001$. r_s= Spearman's rank correlation coefficient.

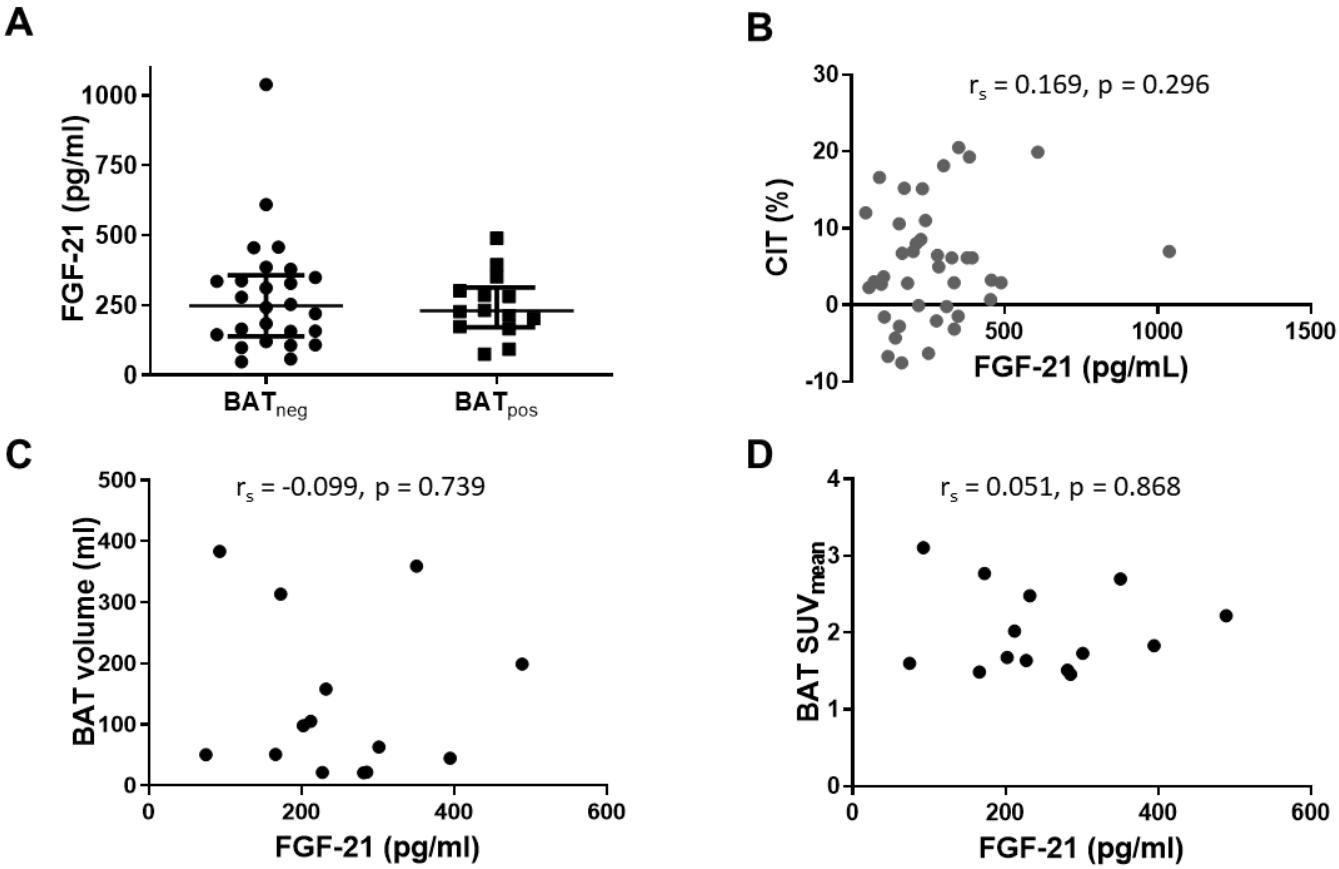

Supplemental Figure 5: No association between circulating FGF-21 and markers of BAT activity. Circulating FGF-21 levels in BAT_{pos} and BAT_{neg} individuals (A). Correlations between FGF-21 and cold-induced thermogenesis (B), BAT volume (C), and BAT glucose uptake (D). r_s= Spearman‘s rank correlation coefficient.

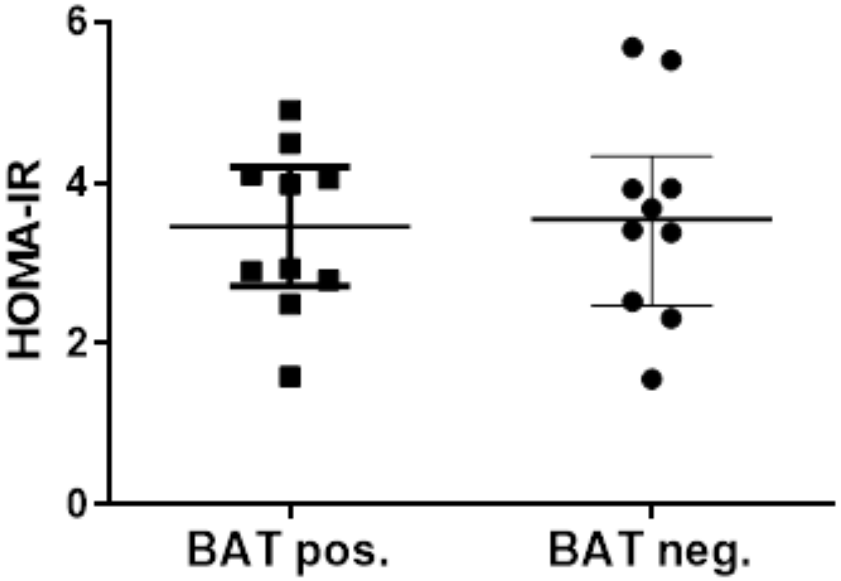

Supplemental Figure 6: HOMA-IR distribution in a subgroup of sex- and HOMA-IR-matched participants (n=10 per group).

	Model 1: unadjusted		Model 2: + age		Model 3: + age & %BF		Model 4: + age & VAT		Model 5: + age & HOMA-IR		Model 6: + age & Outdoor temp.	
	b	**p**	**b**	**p**	**b**	**p**	**b**	**p**	**b**	**p**	**b**	**p**
HOMA-IR*	-0.957	0.009	-0.953	0.014	-0.954	0.016	-0.602	0.102	/	/	-0.924	0.030
Matsuda index*	0.880	0.021	0.847	0.033	0.853	0.036	0.467	0.235	/	/	0.763	0.073
HbA_{1C}	-0.929	0.009	-0.829	0.024	-0.828	0.027	-0.724	0.069	-0.157	0.602	-0.837	0.037
TG*	-0.291	0.396	-0.209	0.562	-0.177	0.622	0.045	0.904	-0.092	0.820	-0.325	0.411
Cholesterol	-0.055	0.880	0.072	0.848	0.137	0.694	-0.053	0.897	-0.211	0.524	0.008	0.984
HDL-C	0.243	0.525	0.341	0.398	0.332	0.418	-0.053	0.891	-0.009	0.984	0.302	0.497
LDL-C	-0.140	0.699	-0.058	0.879	0.024	0.941	-0.168	0.682	-0.310	0.456	-0.091	0.829
CRP*	-0.509	0.167	-0.450	0.245	-0.514	0.159	-0.420	0.321	-0.206	0.624	-0.656	0.119
IL-6*	-0.935	0.007	-0.789	0.020	-0.821	0.013	-0.714	0.049	-0.694	0.064	-0.790	0.036
GGT*	-0.940	0.009	-0.855	0.020	-0.850	0.023	-0.620	0.091	-0.606	0.122	-1.107	0.007
ALAT*	-0.214	0.517	-0.245	0.485	-0.249	0.487	0.043	0.902	-0.002	0.995	-0.336	0.385
ASAT*	-0.685	0.054	-0.773	0.037	-0.771	0.042	-0.657	0.094	-0.785	0.061	-0.891	0.035
ION	-0.958	0.009	-0.934	0.016	-0.933	0.019	-0.540	0.130	0.004	0.962	-0.930	0.029
Liver TBR	-0.780	0.041	-0.745	0.065	-0.724	0.076	-0.646	0.136	-0.543	0.217	-0.621	0.155

Supplemental Table 1: Differences in metabolic parameters between female BAT_{neg} and BAT_{pos} participants only (n=32). %BF: percent body fat; ALAT: alanine aminotransferase; ASAT: aspartate aminotransferase; CRP: C-reactive protein; GGT: gamma-glutamyltransferase; HbA_{1C}: glycated hemoglobin; HDL-C: high-density lipoprotein cholesterol; HOMA-IR: homeostatic model assessment of insulin resistance; ION: Index of NASH; IL-6: interleukin 6; LDL-C: low-density lipoprotein cholesterol, TBR: target-to-background ratio; TG: triglycerides; VAT: visceral adipose tissue. *log-transformed. The regression coefficients (b) depict the effect of the independent variable BAT status (BAT_{neg}=0, BAT_{pos}=1) on each metabolic parameter as the dependent variable. The dependent variables were entered as standardized z-scores.

	BAT_{neg} (n=10)	BAT_{pos} (n=10)	p
HOMA-IR	3.54 (2.53 – 3.93)	3.45 (2.79 – 4.1)	0.880
CIT (%)	2.7 ± 6.4	10.5 ± 6.4	0.013
BMI (kg/m²)	42.4 ± 4.2	41 ± 3.1	0.395
WHR	0.931 ± 0.059	0.876 ± 0.068	0.070
BF (%)	52.5 ± 3.4	52.7 ± 2.5	0.856
Abdominal adipose tissue (ml)	2649 ± 523	2391 ± 406	0.235
SAT (ml)	1933 ± 506	1919 ± 298	0.939
VAT (ml)	715 ± 263	473 ± 182	0.027
CRP (mg/dl)	0.63 (0.26 – 2.15)	0.57 (0.40 – 0.98)	0.880
IL-6 (pg/ml)	5.48 (3.4 – 6.75)	2.22 (1.61 – 3.57)	0.022
Liver TBR	2.03 ± 0.37	1.91 ± 0.26	0.410
GGT (U/l)	24 (18 – 30)	12 (11 – 15)	0.009
ASAT (U/l)	23 (21 – 28)	18 (16 – 21)	0.010
ALAT (U/l)	22 (18 – 23)	20 (17 – 24)	0.596

Supplemental Table 2: Metabolic characteristics of 20 obese individuals matched by HOMA-IR and sex. ALAT: alanine aminotransferase; ASAT: aspartate aminotransferase; BF: body fat; BMI: body mass index; CIT: cold-induced thermogenesis; CRP: C-reactive protein; GGT: gamma-glutamyltransferase; HOMA-IR: homeostasis model assessment of insulin resistance; IL-6: interleukin 6; SAT: abdominal subcutaneous adipose tissue; TBR: target-to-background ratio; VAT: visceral adipose tissue; WHR: waist-to-hip ratio. Data are depicted as counts, mean ± standard deviation, or median (interquartile range), as appropriate.